J. Fluid Mech. (1977), *vol.* 82, *part* 1, *pp.* 29–51
Printed in Great Britain

Influence of the amplitude of a solid wavy wall on a turbulent flow. Part 1. Non-separated flows

By DANIEL P. ZILKER, GERALD W. COOK AND THOMAS J. HANRATTY

Department of Chemical Engineering, University of Illinois, Urbana

(Received 3 September 1976)

Measurements of the shear-stress variation along and the velocity profiles above a solid wavy wall bounding a turbulent flow are presented for waves with height-to-length ratios of $2a/\lambda = 0{\cdot}0312$ and $0{\cdot}05$. These are compared with previous measurements of the wall shear stress reported by Thorsness (1975) and by Morrisroe (1970) for $2a/\lambda = 0{\cdot}012$. The investigation covered a range of conditions from those for which a linear behaviour is observed to those for which a separated flow is just being initiated.

Pressure measurements indicate a linear response in that the spatial variation is described quite well by a single harmonic with a wavelength equal to that of the surface. However, the variation of τ_W for waves with $2a/\lambda = 0{\cdot}0312$ and $0{\cdot}05$ can be more rapid on the leeward side of the wave. The degree of departure from a sinusoidal variation increases with increasing wave height and fluid velocity and, from the results reported in this paper, it is suggested that nonlinear behaviour will become evident when $au^*/\nu \geqslant 27$.

Many aspects of the flow for all three waves are described by a solution of the linear momentum equations previously presented by Thorsness (1975) and by Thorsness & Hanratty (1977). These include the phase and amplitude of the pressure profile and the first harmonic of the shear-stress profile and the velocity field outside the viscous wall region.

These results suggest that up to separation the flow is approximated quite well by linear theory. Nonlinearities affect the flow only in a region very close to the wave surface and are manifested by the appearance of higher harmonics in the variation of τ_W.

1. Introduction

A wavy wall bounding a turbulent flow introduces disturbances which cause spatial variation of the shear and the pressure along the wave surface. Because of the importance of this interaction in determining wave generation on liquid surfaces, sediment transport and flow resistance, considerable attention has been given to the problem of predicting the wave-induced flow over a sinusoidally shaped boundary.

For small enough wave amplitudes a linear response is obtained. This is evidenced by a sinusoidal spatial variation of the wall stress and by a spatially averaged wall shear stress equal to that for a flat surface. For larger amplitude waves the function describing the spatial variation of the wall stress will contain higher-order harmonics and the flow might separate from the leeward side of the wave.

Almost all of the theoretical research on turbulent flow over wavy surfaces has focused on the linear problem. The range of wave amplitudes over which such analyses can be expected to be valid is unknown and experimental measurements are needed both to define this range and to guide much needed theoretical work on flow over waves of finite amplitude. This paper presents results on the influence of wave amplitude on flow of a liquid over trains of sinusoidal waves with a wavelength λ of 5·08 cm. The waves were located on one of the walls of a rectangular channel 5·08 cm high and 60·96 cm wide which was long enough that a fully developed turbulent flow was obtained. The Reynolds number Re based on the half-width of the channel h was varied from 3000 to 32000. Measurements were made of the variation of the shear stress and pressure along the wave surface and of the time-averaged velocity in the direction of mean flow. Measurements were also made of the turbulent velocity fluctuations, but these will be reported in another paper.

In a previous investigation in this laboratory (Thorsness 1975; Thorsness & Hanratty 1977) it was found that a linear response is obtained in this apparatus with waves having a height-to-wavelength ratio $2a/\lambda = 0{\cdot}0125$, where a is the amplitude of the sine function describing the surface. We now compare measurements for waves with $2a/\lambda = 0{\cdot}0312$ and $0{\cdot}05$ with measurements for $2a/\lambda = 0{\cdot}0125$. Dye studies with the $2a/\lambda = 0{\cdot}05$ wave indicated the existence of a very small region of reversed flow close to the solid surface for $Re \lesssim 28000$, but gave no evidence of a large separated region. Consequently, the investigation covered a range of flow conditions from those for which a linear response is obtained to those for which a separated flow is just being initiated.

We find that the assumption of linear behaviour becomes invalid at much smaller amplitudes than would be suggested from pressure measurements; however linear theory is still able to describe many aspects of the flow. For example, it can be used to calculate the first harmonic of the wave-induced flow over the whole range of amplitudes studied and consequently the approximate magnitude of the shear-stress variation. It is also in qualitative agreement with the measured average velocities far from the surface.

Measurements of the pressure variation over sinusoidally shaped waves by Motzfield (1937), Bonchkovskaya (1955), Larras & Claria (1960) and by Zagustin *et al.* (1966) indicate a linear response for $2a/\lambda \leqslant 0{\cdot}05$, i.e. a sinusoidal variation that is approximately 180° out of phase with the wave height. Cook (1970) suggested that shear-stress measurements might be a more sensitive test of the applicability of linear theory. He used electrochemical methods developed in this laboratory (Mitchell & Hanratty 1966; Son & Hanratty 1969) to measure the shear-stress variation along a solid wave with $2a/\lambda = 0{\cdot}05$ and found a nonlinear response, as well as a reversed flow, close to the wave surface. Morrisroe (1970) and later Thorsness (1975) used the techniques developed by Cook to measure the shear-stress variation over a wave with $2a/\lambda = 0{\cdot}0125$ in order to test solutions of the linear momentum equations.

In another series of experiments in this laboratory Zilker (1976) studied waves having height-to-wavelength ratios of 0·0125, 0·0312, 0·05, 0·125 and 0·200. In addition to measuring shear-stress variations along the wave surface, he also measured the time-averaged and fluctuating velocities above the wave surface using a split hot-film sensor and obtained qualitative information about the flow field by studying the motion of injected dye. This paper summarizes the results obtained by Cook and by Zilker for

their waves with $2a/\lambda = 0{\cdot}0125$, $0{\cdot}0312$ and $0{\cdot}05$. Zilker's measurements for $2a/\lambda = 0{\cdot}125$ and $0{\cdot}200$ revealed large separated regions in the flow field and will be discussed in a later paper.

2. Linear analysis

The profiles of the wave surface that were studied are represented in Cartesian co-ordinates as

$$Y_s = a\cos(\alpha x), \tag{1}$$

where a is the amplitude and α the wavenumber. The measurements reported in this paper are the pressure p_W and shear stress τ_W along the wave surface and the component U of the velocity field in the x direction. For a linear system the spatial variation of these quantities is given by

$$\tau_W = \bar{\tau}_W + a|\hat{\tau}|\cos(\alpha x + \theta_\tau), \tag{2}$$

$$p_W = a|\hat{p}|\cos(\alpha x + \theta_p), \tag{3}$$

$$U(Y - Y_s) = \bar{U}(Y) + a|\hat{U}(Y - Y_s)|\cos(\alpha x + \theta_U). \tag{4}$$

The average shear stress $\bar{\tau}_W$ and average velocity $\bar{U}(Y)$ over one wavelength are what would be measured if the wave were replaced by a flat surface. It is to be noted that the location in the flow field is given relative to the wave surface so as to be consistent with the manner in which measurements were made. The amplitudes and phases of p_W, τ_W and U are to be determined from the linear momentum equations.

A number of solutions have appeared in the literature. Helmholtz (1868) neglected the viscous and the Reynolds-stress terms and assumed that the average velocity $\bar{U}$ is constant. A pressure variation at the wave surface is then obtained which is 180° out of phase with the wave. Benjamin (1959) included the effect of viscous terms and took account of the variation of the average velocity in his quasi-laminar analysis. For a solid wave he predicted a shear-stress profile at the wave surface with a maximum upstream of the crest and a pressure profile with a minimum downstream of the crest. More recent solutions of the linear equations have involved attempts at modelling the Reynolds-stress terms. A summary of the results obtained by Thorsness (1975) from his evaluation of a number of approximations of the Reynolds stresses will now be presented.

Thorsness formulated the problem in a boundary-layer co-ordinate system in which the x direction is parallel to the wave surface and the y direction perpendicular to it. Velocities were made dimensionless with respect to a friction velocity $u^* = (\bar{\tau}_W/\rho)^{\frac{1}{2}}$ and lengths with respect to the ratio ν/u^* of the kinematic viscosity to the friction velocity. The stream function

$$\Psi = \int_0^y \bar{U}(y)\,dy + aF(y)\,e^{i\alpha x} \tag{5}$$

is defined such that the wave-induced velocity components in the x and y directions are given by

$$u = h_y^{-1}\,\partial\Psi/\partial y, \quad v = -h_x^{-1}\,\partial\Psi/\partial x, \tag{6}$$

where h_x and h_y are the linearized metric functions for the boundary-layer co-ordinate system:

$$h_x = 1 + a\alpha^2 y\,e^{i\alpha x}, \quad h_y = 1. \tag{7}$$

From the x and y momentum balances the following equation is obtained for F:

$$i\alpha[\bar{U}\{F''-\alpha^2F\}-\bar{U}''F+\alpha^2\bar{U}^2] = [F^{\mathrm{iv}}-2\alpha^2F''+\alpha^4F+2\alpha^2\bar{U}''-\alpha^4\bar{U}]+\mathscr{R}. \quad (8)$$

The terms on the left-hand side are the inertia terms associated with the wave-induced flow, with $\alpha^2\bar{U}^2$ representing a centripetal acceleration associated with the use of a curvilinear co-ordinate system. The terms in the brackets on the right side arise because of viscous stresses. The term $\mathscr{R}$ contains the wave-induced variation of the Reynolds stresses r_{xx} and r_{yy}:

$$\mathscr{R} = i\alpha^3\bar{r}_{xx}+3\alpha\bar{r}'_{xy}+i\alpha(\hat{r}'_{xx}-\hat{r}_{yy})+\alpha^2\hat{r}_{xy}+\hat{r}''_{xy}. \quad (9)$$

Equation (8) is to be solved subject to the boundary condition of zero velocity at the wave surface,

$$F = F' = 0 \quad \text{at} \quad y = 0, \quad (10)$$

and the condition of parallel flow far from the surface,

$$F = \bar{U}, \quad F' = \bar{U}' \quad \text{at large } y. \quad (11)$$

From the solutions the wall shear stress and pressure can be calculated since at $y = 0$

$$p_W = (-ai/\alpha)\,[F'''(0)+\alpha^2\bar{U}'(0)]\,e^{i\alpha x}, \quad (12)$$

$$\tau_W = \bar{\tau}_W + aF''(0)\,e^{i\alpha x}. \quad (13)$$

The reconstruction of the velocity field from the calculated $u(y)$ is discussed in the thesis by Zilker (1976). This requires the recognition that the solution may be visualized as a matching of a solution in boundary-layer co-ordinates to one in Cartesian co-ordinates at a distance y_m from the surface where viscous and turbulent stresses are negligible. Thorsness (1975) found that the viscous and turbulent stresses are important only very close to the boundary and that over most of the region covered by the wave-induced flow the inertia terms on the left side of (8) are dominant. For very large values of α the quasi-laminar assumption of Benjamin (1959), $\mathscr{R} = 0$, gives good results. For $\alpha \to 0$ the pressure variation is given by Kelvin–Helmholtz theory and the shear-stress variation by a pseudo-steady-state assumption. There is a large intermediate range of α for which the calculation of the wave-induced flow depends critically on how the Reynolds stress is modelled.

Thorsness (1975) found an approach used by Loyd, Moffat & Kays (1970) to be useful for this purpose. They neglected the effect of the normal stresses $\bar{r}_{xx}$, $\hat{r}_{xx}$ and $\hat{r}_{yy}$ and used an eddy-viscosity concept to model r_{xy}:

$$r_{xy} = \left(\frac{\bar{\nu}_T(y)}{\nu}+a\frac{\hat{\nu}_T(y)}{\nu}\,e^{i\alpha x}\right)2e_{xy}. \quad (14)$$

Here $\bar{\nu}_T$ is the average eddy viscosity, $a\hat{\nu}_T\,e^{i\alpha x}$ the wave-induced variation, and e_{xy} a component of the rate-of-strain tensor. The van Driest mixing-length equation indicates that

$$\nu_T/\nu = l^2|2e_{xy}| \quad (15)$$

and

$$l = \kappa y[1-\exp(-y\tau_W^{\frac{1}{2}}/A)] \quad (16)$$

for an equilibrium flow. The term κ is the von Kármán constant and $-y\tau_W^{\frac{1}{2}}/A$ is a damping factor which allows for the rapid decrease in the mixing length in the viscous wall region. The thickness of the viscous wall region is governed by the magnitude

of $\tau_W^{\frac{1}{2}}/A$. According to Loyd *et al.* (1970) the term A is a function of the pressure gradient. In an equilibrium flow A, and therefore the thickness of the viscous wall region, increases in regions of favourable pressure gradient and decreases in regions of unfavourable pressure gradient.

For flow over a wavy surface the induced variations in pressure and wall shear stress can cause variations in τ_W and A along the wave surface. If the response of the turbulent boundary layer were instantaneous

$$\tau_W = 1 + a\hat{\tau}_W e^{i\alpha x} \tag{17}$$

and

$$A = \bar{A} + ak_1 \bar{A} i\alpha \hat{p}_W e^{i\alpha x} \tag{18}$$

could be substituted into (16), where $\bar{A}$ is the value of A for a flat wall and k_1 is a parameter representing the influence of the pressure gradient on A for an equilibrium flow. Loyd *et al.* (1970) argue that the response would not be instantaneous, so that relaxation should be considered. Therefore

$$A = \bar{A} + \frac{ak_1 \bar{A} i\alpha \hat{p}_W}{1 + i\alpha k_{LP}} e^{i\alpha x} \tag{19}$$

and

$$\tau_W = 1 + \frac{a\hat{\tau}_W}{1 + i\alpha k_{L\tau}} e^{i\alpha x} \tag{20}$$

are introduced into (16) rather than (17) and (18). The following equation for $\hat{\nu}_T$ is obtained for small amplitude waves:

$$\frac{\hat{\nu}_T}{\bar{\nu}_T} = \frac{F'' + \alpha^2 F - \alpha^2 \bar{U}}{\bar{U}'} + \left(\frac{2\exp(-y/\bar{A})}{1 - \exp(y/\bar{A})}\right)\frac{y}{\bar{A}} \times \left(\frac{F''(0)}{2(a + i\alpha k_{L\tau})} - \frac{k_1 \bar{A} i\alpha \hat{p}}{1 + ik_{LP}}\right). \tag{21}$$

The correlations presented by Loyd *et al.* (1970) suggest that $\kappa = 0{\cdot}41$, $\bar{A} = 25$, $k_1 = -30$, $k_{LP} = 3000$ and $k_{L\tau} = 0$. Thorsness found that somewhat better agreement with measurements of wall stress could be obtained using $k_1 = -60$, $k_{LP} = 3000$ and $k_{L\tau} = 0$. This is referred to as model D in the thesis by Thorsness.

3. Description of experiments

The flow loop

The experiments were conducted in the flow loop sketched in figure 1. The 8·38 m rectangular channel through which the electrolyte was circulated had inside dimensions of 5·08 cm by 60·96 cm. The inlet to the channel was preceded by a 91·4 cm long round-to-rectangular diffuser section and a 7·6 cm long honeycomb contained in the 15·24 cm pipe at the inlet to the diffuser.

The honeycomb was constructed by taking a 20·3 cm diameter piece of Plexiglas and drilling 1·27 cm diameter holes in it as close together as possible. Each hole was countersunk, thus presenting only sharp edges to the approaching flow. The end result simulated a tube bundle in a closely packed arrangement with each tube having a length-to-diameter ratio of six. A calming section consisting of 53·4 cm length of 15·2 cm pipe was placed between the honeycomb and the diffuser.

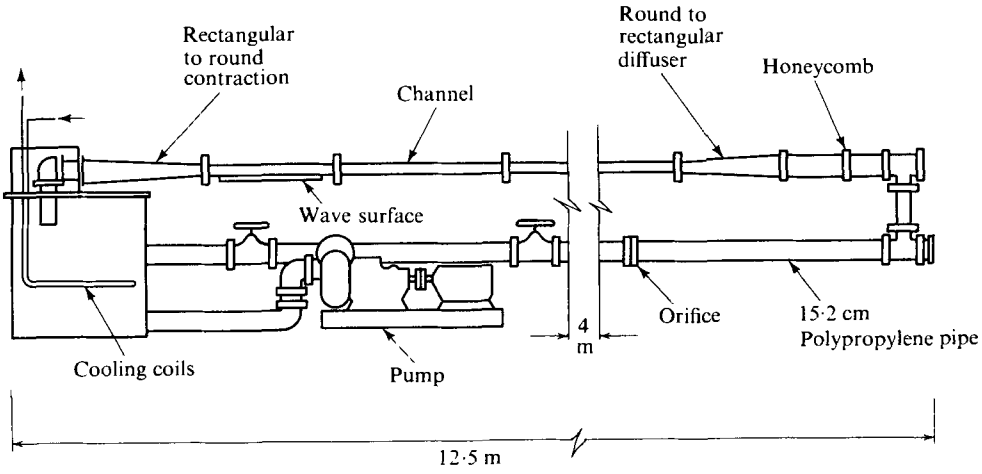

FIGURE 1. Rectangular channel flow loop.

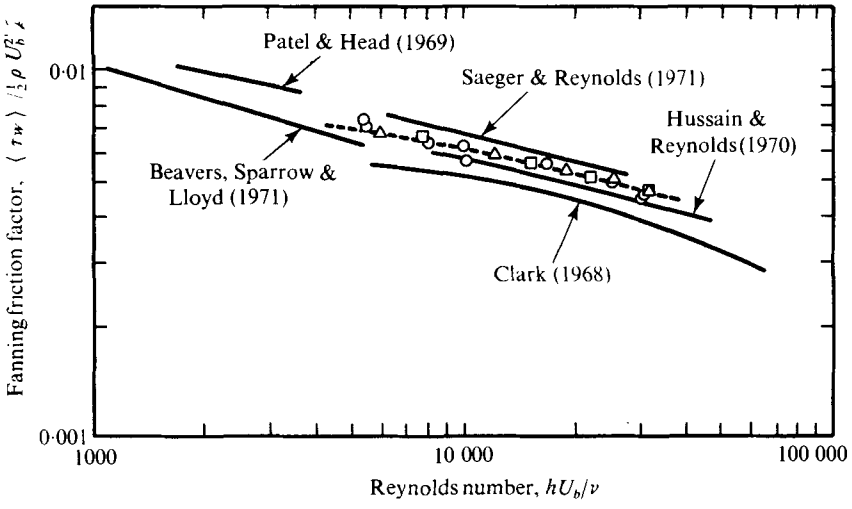

FIGURE 2. Fanning friction factor. ○, $2a/\lambda = 0{\cdot}0125$; □, $2a/\lambda = 0{\cdot}0312$; △, $2a/\lambda = 0{\cdot}05$; ---, flat channel.

The test section was located at the downstream end of the rectangular channel. The bottom portion consisted of a removable 60·96 cm by 68·58 cm test plate which contained the waves to be studied.

Preliminary tests were conducted with a flat surface in the test section to see how closely the flow approximated fully developed channel flow. Velocity measurements made at $yu^*/\nu \geqq 30$ by Zilker (1976) for large flow rates exhibit the logarithmic behaviour

$$\frac{\bar{U}}{u^*} = \frac{1}{0{\cdot}41} \ln\left(\frac{yu^*}{\nu}\right) + 5{\cdot}1 \tag{22}$$

suggested by Kline, Morkovin & Cockrell (1969).

The orifice plate used to measure flow rates was calibrated by integrating these velocity profiles. A bulk velocity U_b is defined as if the velocity profile at the centre of the channel existed over the whole cross-section:

$$U_b = \frac{1}{h}\int_0^h \overline{U}\, dy, \tag{23}$$

where h is the half-width of the channel and $\overline{U}$ is the average velocity at a distance y from the test surface. The Reynolds number used to characterize the flow is then $Re = hU_b/\nu$.

Thorsness (1975) measured the wall shear stress $\overline{\tau}_W$ on a flat plate using the electrochemical techniques to be described later in this section. From these he calculated the skin-friction factor

$$f = \overline{\tau}_W/\tfrac{1}{2}\rho U_b^2. \tag{24}$$

As may be seen in figure 2 these compare reasonably well with values obtained in a number of other laboratories using pressure-drop measurements in the fully developed region.

The wave sections

Five different wavy test surfaces with $2a/\lambda$ values of 0·0125, 0·03125, 0·05, 0·125 and 0·200 were constructed from Plexiglas. All of these had ten crests separated by a distance of 5·08 cm. Different methods were used to fabricate the wave surfaces. Those with $2a/\lambda = 0{\cdot}05$ and with $2a/\lambda = 0{\cdot}200$ are described by Cook (1970) and by Zilker (1972). The method used for the other three wave surfaces was found to be superior from the viewpoint of controlling wave dimensions and will be described here.

A wave-surface cutting tool covering one wavelength was constructed using a vertical end mill which was moved an appropriate distance in the vertical direction while progressing incremental distances in the horizontal direction as small as 0·00254 cm. The radius of curvature of the end mill and the radius of curvature of the surface were input parameters to a tool design program. The output from this program was used by the machinist to make the correct moves along the sinusoidal tool profile. Four of these tools were then placed in a rotary-cutter assembly and used in a manner described by Cook (1970). Wavy surfaces produced from these high precision tools required little finishing work. This consisted merely of smoothing the surfaces with progressively finer grades of sandpaper and polishing with DuPont 0861N Rubbing Compound and DuPont 0761N Polishing Compound.

The wavy sections were constructed such that the mean wave height was in the same plane as a flat channel section over which the preliminary measurements were made. Holes were drilled in the surface for platinum wires of various diameters used in the shear-stress measurements and for pressure taps. After the electrodes had been glued in place with epoxy cement the surfaces were repolished as described above.

Shear-stress measurements

The wall shear stresses along the wave surface were measured by an electrochemical method which is the mass-transfer analogue of the constant-temperature hot-film anemometer. A chemical reaction occurs on an electrode embedded flush with the surface of the wave. The voltage on the electrode is so adjusted that the rate of

chemical reaction is large enough that the concentration of reacting species on the surface of the electrode is constant and equal to zero, i.e. the reaction rate is mass-transfer controlled. The current I flowing in the electrochemical circuit is then related to the mass-transfer coefficient K and the concentration C_b of the reacting species in the bulk fluid through the equation

$$K = I/n\mathscr{F}AC_b, \tag{25}$$

where n is the number of electrons involved in the reaction, $\mathscr{F}$ is Faraday's constant and A is the area of the electrode. For a two-dimensional flow over a circular electrode surface Jolls & Hanratty (1969) have shown from a solution of the mass balance equation that the wall shear stress τ_W is related to K by the equation

$$\tau_W = \left(\frac{2\Gamma(\frac{4}{3})K^3}{3}\right)\frac{9L_e\mu}{D^2}, \tag{26}$$

where μ is the viscosity of the fluid, D the diffusion coefficient for the reacting species and L_e the equivalent length of the electrode, equal to 0·816 times the diameter of the electrode. The assumptions made in the derivation of (26) are that molecular diffusion in the lateral direction and in the direction of flow can be neglected and that the velocity field within the concentration boundary layer is given by

$$u = (\tau_W/\mu)y. \tag{27}$$

The neglect of molecular diffusion in the lateral direction compared with that in the direction perpendicular to the electrode surface requires that the thickness of the concentration boundary layer on the electrode surface is small compared with the width of the electrode. This is well justified for the experiments reported in this paper, for which this ratio is 0·036. Molecular diffusion in the direction of flow can be neglected provided that the group $\tau_W L_e^2/\mu D$ is small. From discussions presented by Dimopoulos & Hanratty (1968) we conclude that errors associated with the neglect of diffusion in the flow direction and with assumption of a velocity profile of the form (27) can be significant only in some very small neighbourhood of a separation or a reattachment point. This follows since the concentration boundary layer over the test electrode is so thin, about 0·046 times the thickness of the viscous sublayer for the experiments reported in this paper.

Since (26) was derived for a two-dimensional flow its application to a turbulent flow requires that the transverse component τ_z' of the fluctuating stress is small compared with the time-averaged stress $\bar{\tau}_W$. If the transverse fluctuating component can be neglected then

$$I = C(\bar{\tau}_W + \tau_x')^{\frac{1}{3}}, \tag{28}$$

where C is a proportionality constant. Then, if it is assumed that $(\tau_x'/\bar{\tau}_W)^2 \ll \tau_x'/\bar{\tau}_W$, the right side can be expanded to give

$$\bar{I} = C\bar{\tau}_W^{\frac{1}{3}}, \tag{29}$$

$$(I - \bar{I})/\bar{I} = C\tfrac{1}{3}\tau_x'/\bar{\tau}_W. \tag{30}$$

Another approach is to measure the cube of the current. Then

$$\overline{I^3} = C^3\bar{\tau}_W, \quad I^3 - \overline{I^3} = C^3\tau_x'. \tag{31), (32}$$

Viscosity (P)	0·0087
Density (g/cm³)	1·023
Kinematic viscosity (cm²/s)	0·00867
Mass diffusivity (cm²/s)	$1{\cdot}146 \times 10^{-5}$
Schmidt number	756
KI concentration (moles/l)	0·103–0·2
I_2 (I_3^-) concentration (moles/l)	0·00135–0·00145
Temperature (°C)	25·0

TABLE 1. Physical and chemical properties of the electrochemical solution.

The application of (29) then implies that the fluctuations are small enough that $\bar{I}^3 = \overline{I^3}$. For circumstances under which the above condition is not satisfied it is quite likely that the neglect of the influence of the transverse component of the fluctuating stress is also not justified. From dye studies to be described later and from a comparison of measurements of $\bar{I}^3$ and $\overline{I^3}$, we conclude that the presence of large transverse velocity fluctuations prevents accurate measurements of the wall shear stress in the neighbourhood of a separation point or in a region where a separated zone of large dimensions exists.

The redox reaction used in this study is the potassium iodide and iodine reaction system, in which the following reactions occur:

$$I_3^- + 2e^- \rightarrow 3I^- \quad \text{(cathode)},$$
$$3I^- \rightarrow I_3^- + 2e^- \quad \text{(anode)}.$$

The approximate concentrations of the I_3^- and the potassium iodide supporting electrolyte were 0·0015 M and 0·2 M respectively. The properties of the electrolyte are summarized in table 1. The diffusion coefficients for the iodine to be used in (26) were calculated from a correlation developed by Shaw (1976):

$$\log_{10} D = 1{\cdot}07291 \log_{10} \nu - 7{\cdot}15278, \tag{33}$$

where ν is the kinematic viscosity.

Local time-averaged shear stresses were obtained by using 0·051 cm diameter platinum wires located every 0·254 cm in the direction of mean flow while 0·0102 cm electrodes were used to measure the local root-mean-square value of the fluctuating shear stress. The diameter of the electrodes used for fluctuating measurements was small enough that according to considerations presented by Shaw (1976) no spatial averaging occurred on their surfaces.

Figures 3 and 4 show the locations of the electrodes in the wave surfaces with $2a/\lambda = 0{\cdot}03125$ and with $2a/\lambda = 0{\cdot}05$. The paper by Thorsness (1975) shows the electrode arrangement for the $2a/\lambda = 0{\cdot}0125$ wave. The platinum wires were glued in place with epoxy cement and sanded flush with the surface using the procedure outlined in the previous section. These electrodes were the cathode of an electrolysis cell. The anode consisted of an approximately 1000 cm² nickel sheet completely immersed in the solution. The much smaller area of the cathode surface ensured that the current flow was controlled by processes occurring at the test electrode.

Considerably more detail about the electrochemical techniques used for these measurements can be found in a number of previous publications from this laboratory.

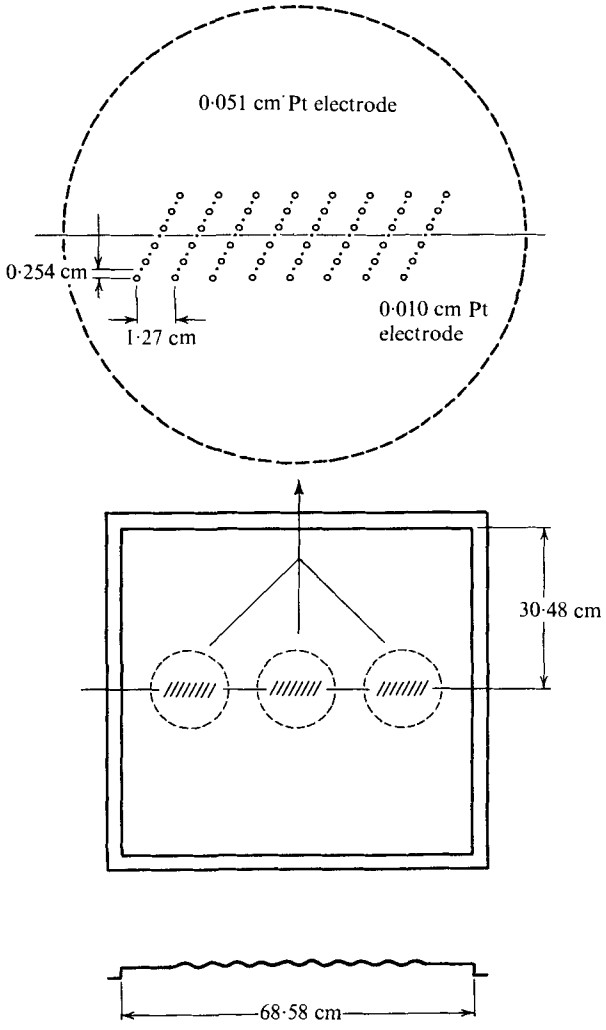

FIGURE 3. Electrode configuration on $2a/\lambda = 0{\cdot}0312$ wave surface.

Mitchell & Hanratty (1966), Hanratty (1967) and Sirkar & Hanratty (1970) have described their use to measure the fluctuating wall velocity gradient for fully developed turbulent flow in a pipe and Son & Hanratty (1969) and Dimopoulos & Hanratty (1968) their use to study flow around a cylinder. Fortuna & Hanratty (1971) have analysed their frequency response.

Measurement of pressure profiles

The time-averaged pressure profile along the wave surface with $2a/\lambda = 0{\cdot}05$ was measured using the pressure taps shown in figure 4. These 0·084 cm diameter holes were drilled in three groups of twenty along the waves on which electrochemical measurements were made. The holes were enlarged to 0·325 cm on the back side to accommodate stainless-steel tubes which were connected to a CGS Datametrics Model 550–5, 0–10 psid differential pressure transducer.

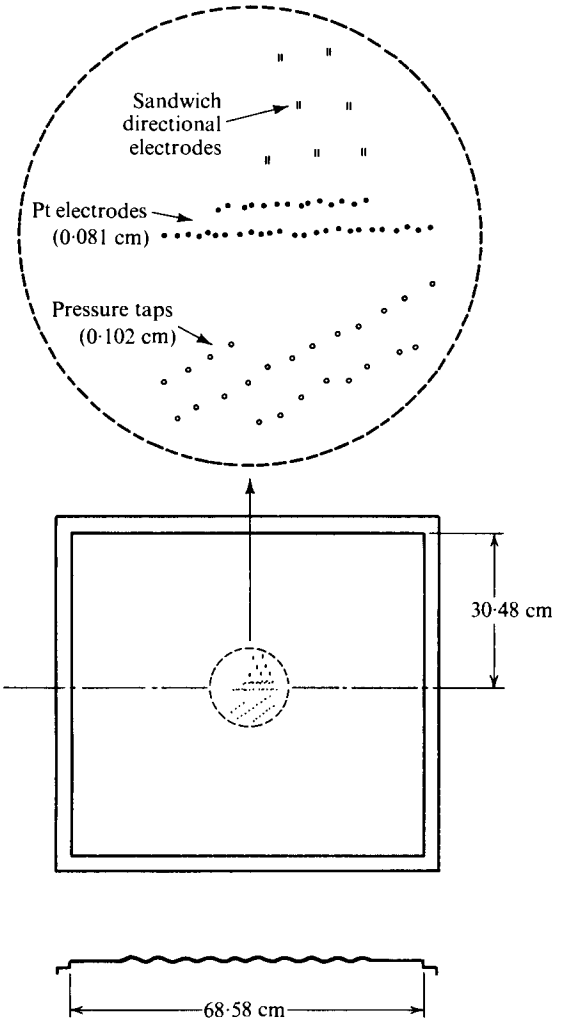

FIGURE 4. Electrode and pressure-tap configuration on $2a/\lambda = 0{\cdot}05$ wave surface.

Measurement of flow direction

The electrode measurements gave only the magnitude of the shear stress. Since reversed flows existed close to the surface of the $2a/\lambda = 0{\cdot}05$ wave, independent experiments had to be performed to determine a sign for the shear stress. One of these involved the injection of dye through the pressure taps. The other used the sandwich electrodes developed by Son & Hanratty (1969) to determine the separation point for flow around a cylinder.

These consisted of two rectangular electrodes sandwiched together with a thin layer of insulation and mounted in the wave surface with their long side perpendicular to the direction of mean flow. The difference in the signal from the two electrodes indicates the flow direction, since a smaller mass transfer rate is registered by the downstream electrode.

The procedure followed in using these electrodes was to activate each electrode individually and record its average current. Then both electrodes were activated

simultaneously and their currents recorded. The flow direction was determined by the electrode which had the largest percentage change in the electrochemical cell current between the two above conditions.

Velocity measurements

Measurements of the average velocity and the root-mean-square values of two components of the turbulent velocity fluctuations were obtained over a flat surface and over the wave surfaces using a Thermo-Systems, Inc., 1287-EW split film sensor. The probe was operated in the constant-temperature mode using a Thermo-Systems Model 1050 anemometer module and a Thermo-Systems Model 1051–6 power supply module. In this paper we report only on the average velocity measurements.

The probes were calibrated using the towing tank and the liquid jet facility described in the thesis by Zilker (1976). The calibration data were analysed using a method suggested by Blinco & Sandborn (1973).

The probe was attached to a traversing mechanism which entered the channel from its top surface. Provisions were made to position the traversing mechanism at ten different locations between the eighth and tenth wave crests. The positions from 0 to $0{\cdot}4x/\lambda$ were located every $0{\cdot}1x/\lambda$ from the eighth wave crest. The remaining traversing positions from 0·5 to $0{\cdot}9x/\lambda$ were similarly located along the ninth wave. At each location the probe was traversed until its boundary protection pins touched the wavy surface, which established the split hot-film probe's exact location above the surface. The probe's sensors were then activated, and two minutes of analog probe data were recorded using a Sangamo Model 3600 14 track FM tape recorder. This procedure was repeated as the probe was moved away from the solid boundary. Data from the split hot-film probe were subsequently analysed by an IBM/1800 computer which sampled each segment of analog data, converted these samples to 16 bit digital numbers, and then processed these digital data to obtain the required velocity-field information.

4. Results

Characterization of the flow

The goal of the experiments was to study flow over a portion of a wave train where a periodic pattern existed. This did not pose a serious problem since the flow established itself rather rapidly.

Cook (1970) carried out preliminary pressure measurements over a train of 24 waves with $2a/\lambda = 0{\cdot}05$. As can be seen in figure 17 of his thesis no difference could be found between pressure distributions over the sixth and fourteenth wave. A more sensitive test is obtained from the profiles of wall shear stress.

Zilker (1976) carried out measurements of the wall stress profile over the first, second, fifth, sixth, ninth and tenth waves of a train of ten waves having a height-to-length ratio of $2a/\lambda = 0{\cdot}0312$. No significant change in the shear-stress profile could be discerned after the second wave.

Profiles of wall shear stress

Measurements of the variation of the shear stress along waves with $2a/\lambda = 0{\cdot}03125$ and with $2a/\lambda = 0{\cdot}05$ are shown in figures 6 and 7. Local average shear-stress data for

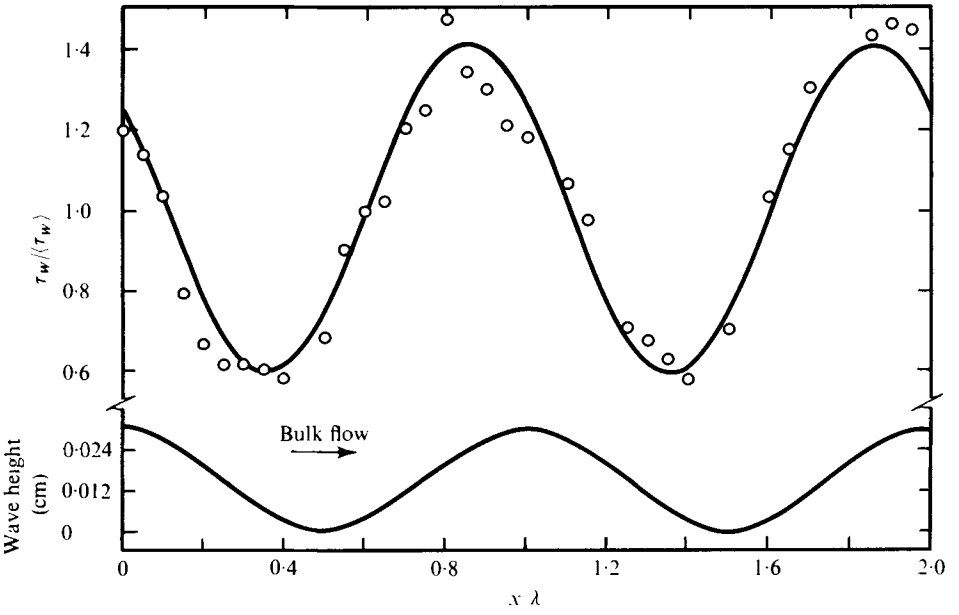

FIGURE 5. Shear-stress distribution over $2a/\lambda = 0{\cdot}0125$ wave surface at $Re = 9680$. ——, first harmonic. $\alpha\nu/u^* = 0{\cdot}00584$, $au^*/\nu = 6{\cdot}7$.

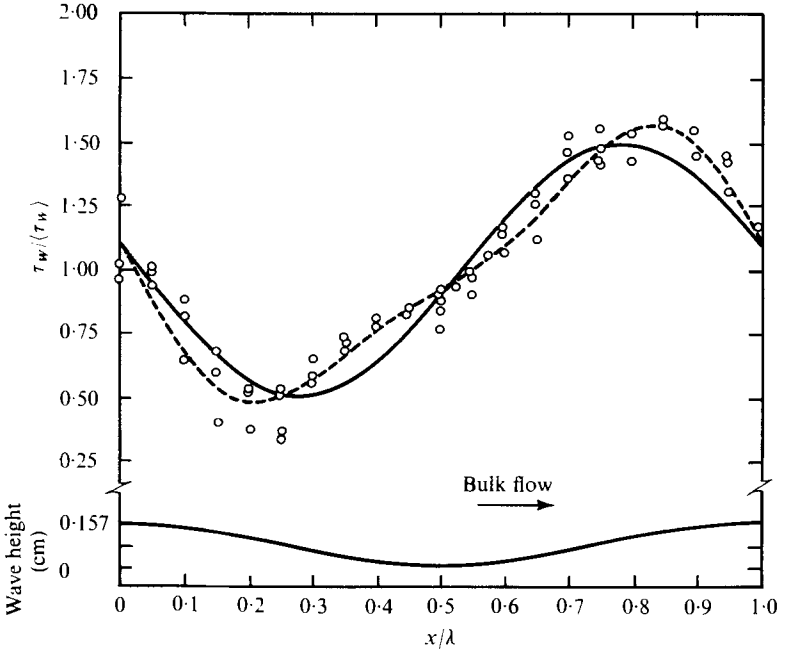

FIGURE 6(*a*). For legend see next page.

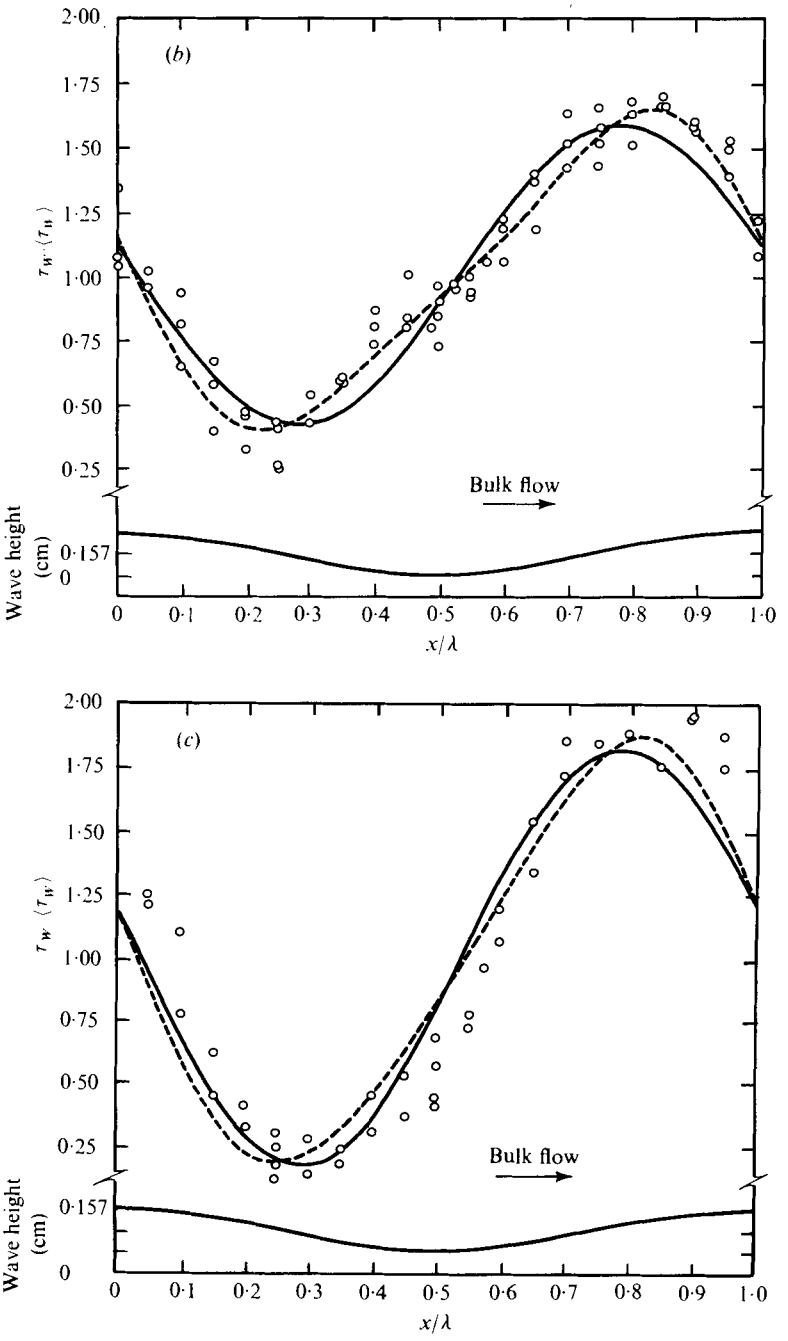

FIGURE 6. Shear-stress distributions over $2a/\lambda = 0{\cdot}0312$ wave surface. ——, first harmonic; – – –, first and second harmonic. (*a*) $Re = 31000$, $a\nu/u^* = 0{\cdot}00195$, $au^*/\nu = 50{\cdot}5$. (*b*) $Re = 15200$, $a\nu/u^* = 0{\cdot}00363$, $au^*/\nu = 27{\cdot}0$. (*c*) $Re = 7850$, $a\nu/u^* = 0{\cdot}00656$, $au^*/\nu = 14{\cdot}9$.

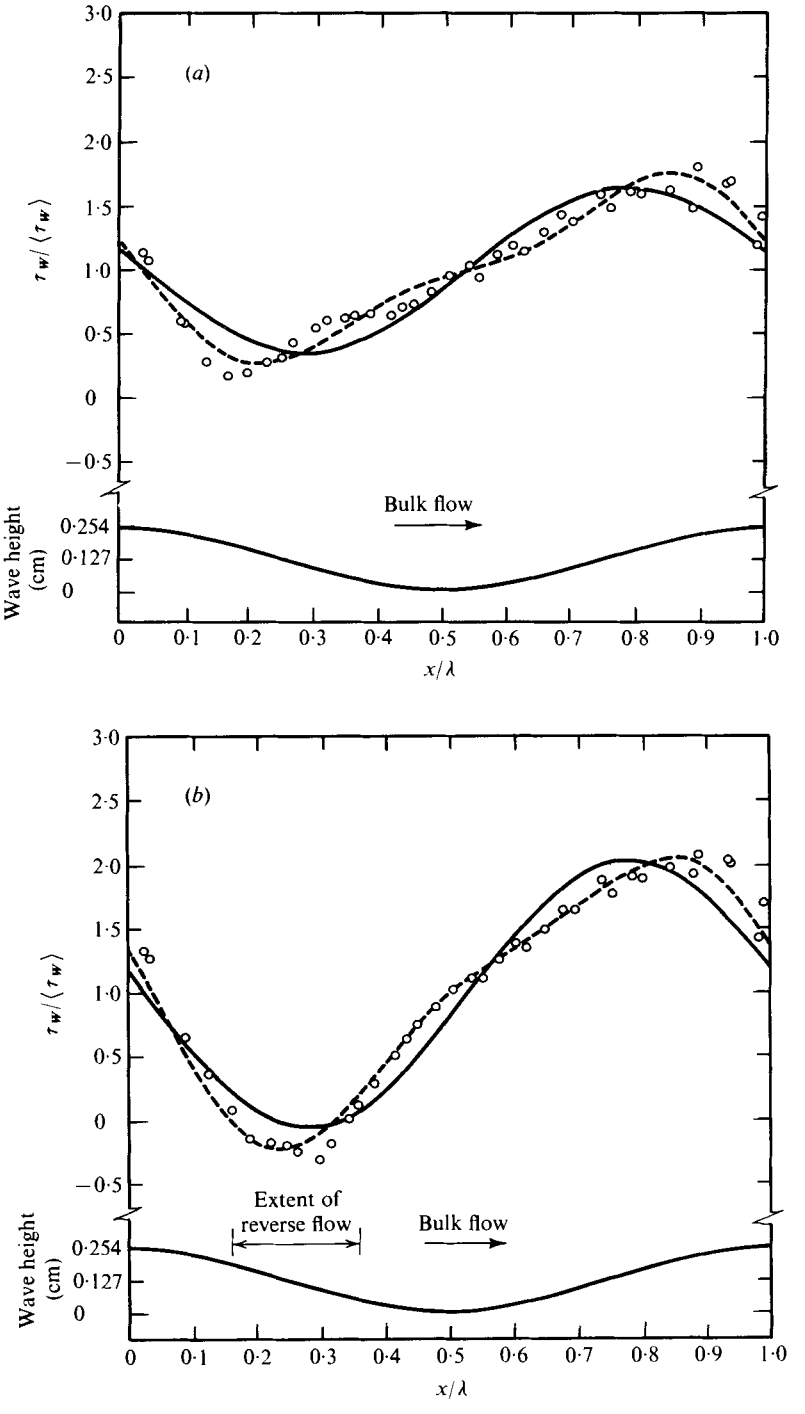

FIGURES 7(*a*, *b*). For legend see next page.

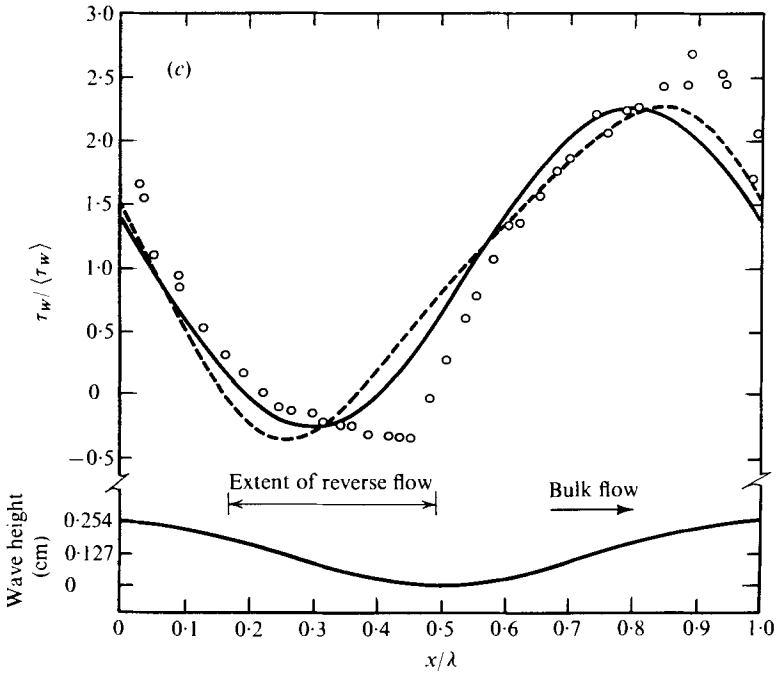

FIGURE 7. Shear-stress distributions over $2a/\lambda = 0{\cdot}05$ wave surface. ——, first harmonic; ---, first and second harmonic. (*a*) $Re = 31840$, $\alpha\nu/u^* = 0{\cdot}00195$, $au^*/\nu = 80{\cdot}3$. (*b*) $Re = 19260$, $\alpha\nu/u^* = 0{\cdot}00303$, $au^*/\nu = 51{\cdot}9$. (*c*) $Re = 6020$, $\alpha\nu/u^* = 0{\cdot}00856$, $au^*/\nu = 18{\cdot}3$.

the $2a/\lambda = 0{\cdot}05$ wave were plotted as positive or negative depending on the flow direction determined from the studies outlined in the previous section. For comparison one of the profiles obtained by Thorsness with a $2a/\lambda = 0{\cdot}0125$ wave, for which a linear response is obtained, is shown in figure 5.

The abscissae of these figures are the ratio $\tau_W/\langle\tau_W\rangle$, where τ_W is the local wall shear stress and $\langle\tau_W\rangle$ is the average over one wavelength. The curves are plots of the function

$$\frac{\tau_W}{\langle\tau_W\rangle} = \sum_{n=0}^{N} a_n \sin\left(\frac{2\pi n x}{\lambda}\right) + b_n \cos\left(\frac{2\pi n x}{\lambda}\right) \tag{34}$$

with $N = 1$ or 2.

Figure 5 shows that the measurements for $2a/\lambda = 0{\cdot}0125$ are fitted quite well by a curve with a single harmonic which is 51° out of phase with the wave profile. Of particular interest is the large amplitude of wall stress variation obtained with such a small wave.

An increase in the wave amplitude to $2a/\lambda = 0{\cdot}0312$ (figure 6) causes an observable departure from a linear response in the wall shear-stress variation. This is evidenced by a more gradual variation of the wall shear stress on the leeward than on the windward side of the wave. The degree of departure from linear behaviour is found to increase with increasing flow rate. It is noted that some improvement in the fit of the data is obtained by using a curve with two harmonics at $Re = 31000$ and at $Re = 15200$. However, at $Re = 7850$, where the response is close to linear, not much improvement is obtained.

$2a/\lambda$	Re	$\alpha^+ = \alpha\nu/u^*$	$a^+ = au^*/\nu$	C_2/C_1
0·0125	30460	$2{\cdot}12 \times 10^{-3}$	18·5	0·073
	20880	$2{\cdot}95 \times 10^{-3}$	13·3	0·059
	9680	$5{\cdot}84 \times 10^{-3}$	6·7	0·032
	5420	$9{\cdot}85 \times 10^{-3}$	4·0	0·025
0·0312	31010	$1{\cdot}95 \times 10^{-3}$	50·5	0·261
	22840	$2{\cdot}54 \times 10^{-3}$	38·6	0·215
	15220	$3{\cdot}63 \times 10^{-3}$	27·0	0·116
	7850	$6{\cdot}56 \times 10^{-3}$	14·9	0·064
0·050	31840	$1{\cdot}95 \times 10^{-3}$	80·3	0·317
	24740	$2{\cdot}43 \times 10^{-3}$	64·6	0·230
	19260	$3{\cdot}03 \times 10^{-3}$	51·9	0·184
	11940	$4{\cdot}62 \times 10^{-3}$	33·0	0·159
	6020	$8{\cdot}56 \times 10^{-3}$	18·3	0·098

TABLE 2. Harmonic coefficient ratios of wavy-surface shear stress.

As can be seen in figure 7, an increase in the wave amplitude to $2a/\lambda = 0{\cdot}05$ can cause an even greater distortion of the shear-stress profile. Regions of reverse flow close to the surface are found for $Re = 7200$ and for $Re = 16100$ but not for $Re = 32000$. These are located on the downstream portion of the wave midway between the crest and the trough.

For all three waves the degree of departure from linearity increases with increasing fluid velocity, even though the amplitude of the variation of the wall shear stress decreases. This is further illustrated in table 2, where the amplitudes of the harmonics, defined from (34) as

$$C_i^2 = a_i^2 + b_i^2, \tag{35}$$

have been calculated from a Fourier analysis. It is noted that an increase in the magnitude of the second harmonic is obtained by increasing either the wave amplitude or the fluid velocity.

A comparison of table 2 with figures 5–7 indicates that an observable difference from a sinusoidal variation is obtained when the Fourier analysis gives $C_2/C_1 \geqslant 0{\cdot}116$. Consequently it is concluded that significant departures from linear behaviour occur when $au^*/\nu \geqslant 27$.

Pressure profiles

The behaviour of the wall shear-stress profiles observed in this research is of interest since previous measurements of pressure profiles indicate a linear response for $2a/\lambda \leqslant 0{\cdot}05$. Therefore we carried out measurements of pressure profiles on the wave with $2a/\lambda = 0{\cdot}05$ for Reynolds numbers from 5650 to 30000 to see whether a linear response in the pressure variation is also found in our equipment. One of these measured profiles is shown in figure 8. Results from these experiments are consistent with the findings of previous investigators in that all of the measured profiles may be fitted with a curve having a single harmonic.

Influence of wave amplitude on the first harmonic and on $\langle \tau_W \rangle$

The influence of the wave amplitude on the amplitude of the first harmonic of the shear-stress variation and on $\langle \tau_W \rangle$ is shown in figures 2 and 9. The skin-friction

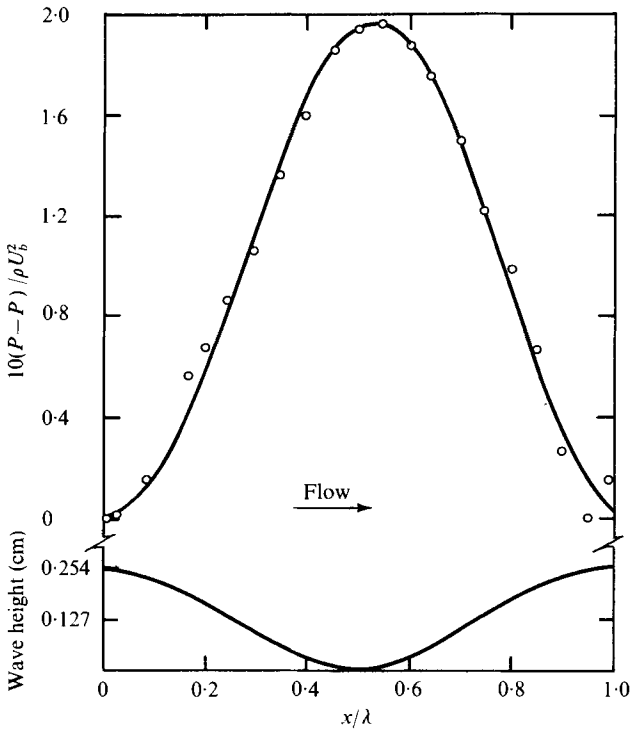

FIGURE 8. Pressure distribution over $2a/\lambda = 0{\cdot}05$ wave surface at $Re = 15060$. ——, first harmonic.

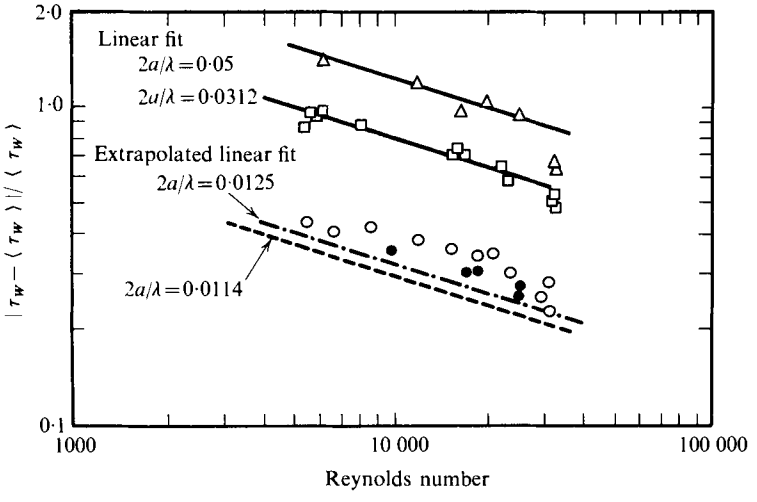

FIGURE 9. Magnitude of shear-stress fluctuations as a function of Reynolds number. ●, $2a/\lambda = 0{\cdot}0114$; ○, $2a/\lambda = 0{\cdot}0125$; □, $2a/\lambda = 0{\cdot}0312$; △, $2a/\lambda = 0{\cdot}050$.

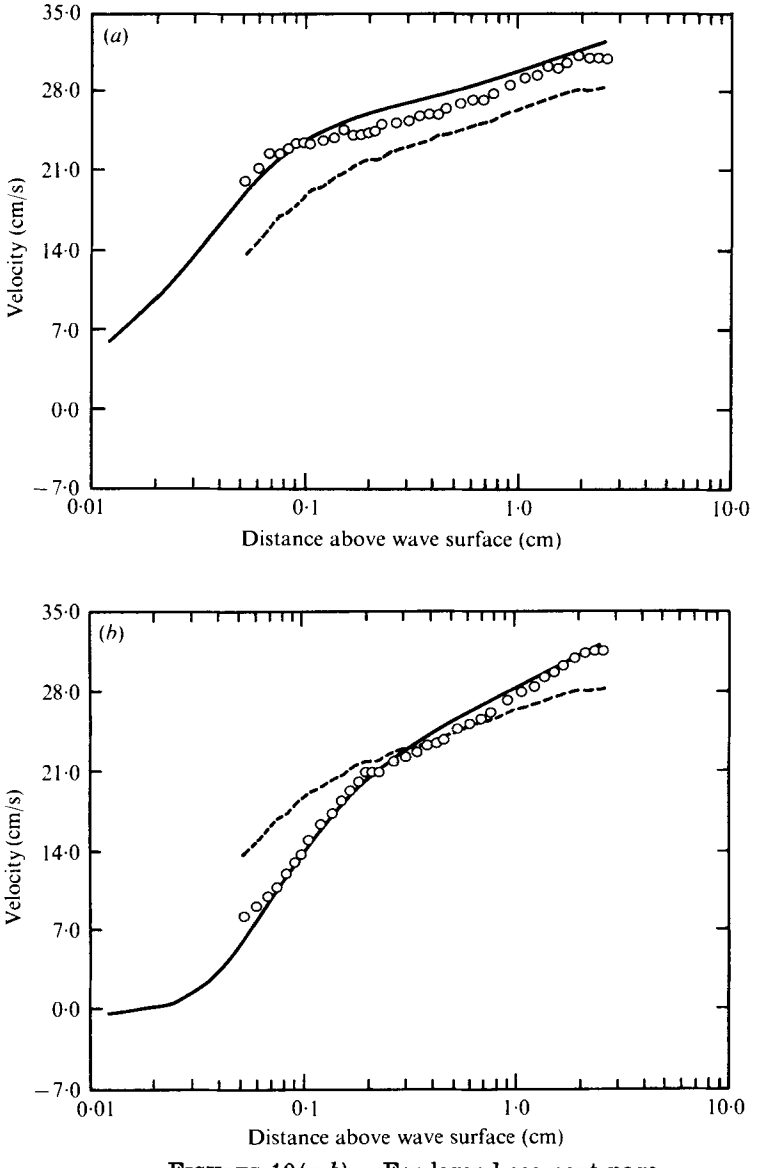

FIGURES 10(*a*, *b*). For legend see next page.

coefficients $f_s = \langle \tau_W \rangle / \frac{1}{2}\rho U_b^2$ shown in figure 2 for the three waves agree within experimental error with the measurements obtained with a flat plate. This type of result is what would be expected for a linear behaviour.

Further evidence that many aspects of the flow may be described by linear theory is given in figure 9, where the amplitude $(a_1^2 + b_1^2)^{\frac{1}{2}}$ of the first harmonic of the function describing the variation of $\tau_W / \langle \tau_W \rangle$ is plotted. The relative magnitudes of the first harmonics for the two larger amplitude waves indicate a linear dependence on a, as shown by the two solid lines. The extrapolations of this linear relation to the waves with $2a/\lambda = 0{\cdot}0114$ and with $2a/\lambda = 0{\cdot}0125$ are given by the two broken lines in figure 9. Approximate agreement is noted. In fact the differences are of the magnitude

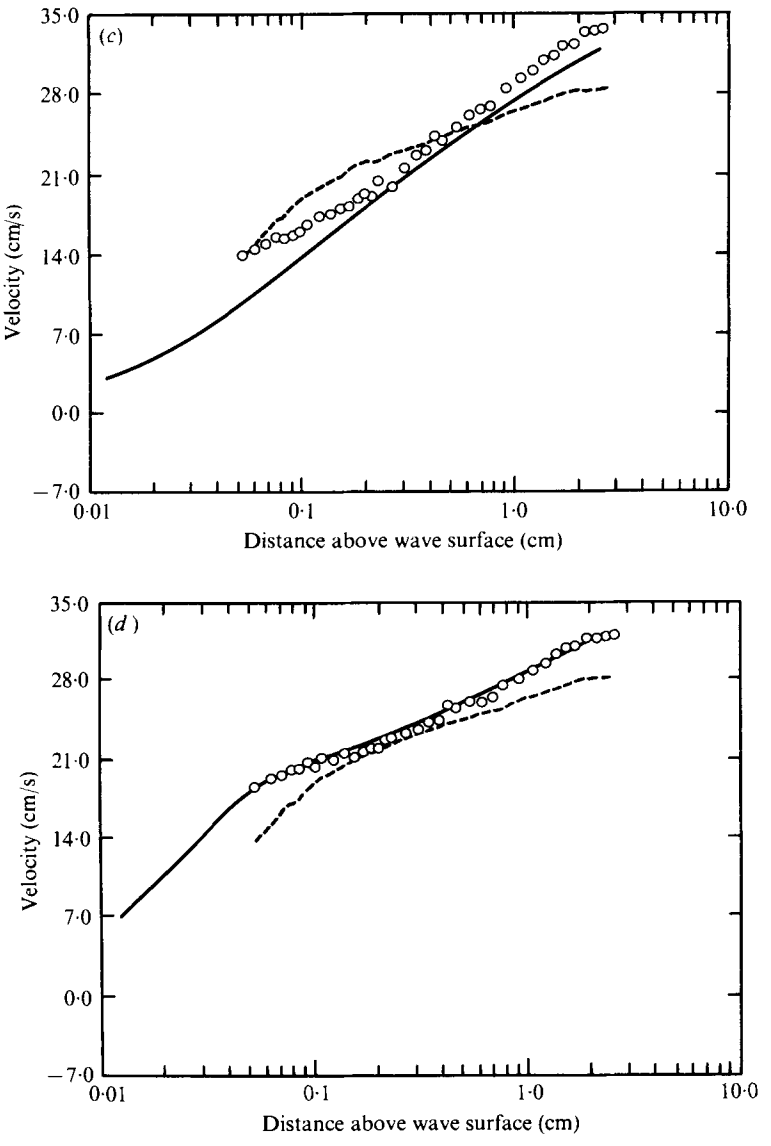

FIGURE 10. Average velocity profiles over $2a/\lambda = 0{\cdot}05$ wave surface at (*a*) $x/\lambda = 0$ ($\tau_W/\langle\tau_W\rangle \simeq 1{\cdot}5$), (*b*) $x/\lambda = 0{\cdot}3$ ($\tau_W/\langle\tau_W\rangle \simeq -0{\cdot}2$), (*c*) $x/\lambda = 0{\cdot}6$ ($\tau_W/\langle\tau_W\rangle \simeq 1{\cdot}0$) and (*d*) $x/\lambda = 0{\cdot}8$ ($\tau_W/\langle\tau_W\rangle \simeq 2{\cdot}2$). ——, model *D*; – – –, flat channel; ○, $\bar{U}$.

which would be expected for errors in the measured amplitude of the wave surface of 0·00508 cm.

Velocity measurements

The measured velocity profiles at different locations along the wave surface are shown in figure 10 for a wave with $2a/\lambda = 0{\cdot}05$. The abscissa in these curves is the distance above the wave surface at that location. The velocity is the time-averaged velocity in the direction of mean flow. For comparison, data obtained with a flat plate at a bulk velocity of 25 cm/s are also shown. It is noted that in the neighbourhood of the wave

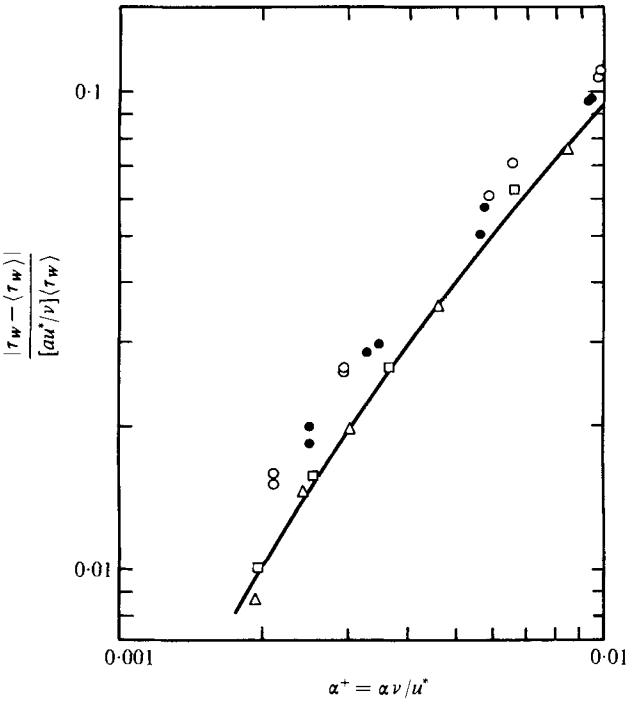

FIGURE 11 (*a*). For legend see next page.

crest the shape of the velocity profile is similar to that for a flat wall but that in the trough region profiles with shapes quite different from those for a flat plate are obtained.

5. Comparison of the measurements with calculations based on linear theory

The remarkable qualitative agreement of many of the aspects of our experimental results with what would be expected for a linear response suggested that we make a quantitative comparison. For this purpose we used the model for the wave-induced variations of the Reynolds stresses developed by Thorsness (1975) and discussed in § 2.

The curves shown in figures 11 (*a*) and (*b*) are the calculated amplitude and phase of the wall shear-stress variation. Here the first harmonic of $|\tau_W - \langle \tau_W \rangle|/\langle \tau_W \rangle$ has been normalized with the dimensionless wave amplitude au^*/ν and plotted against the dimensionless wavenumber $a\nu/u^*$. The solid curves shown in figure 10 are the velocity profiles calculated from linear theory. The agreement between calculations and measurements is within the accuracy that can be expected from the approximate model of the Reynolds stresses developed by Thorsness (1975).

Thorsness also compared a solution of the linear momentum equations using his model *D* for the Reynolds stress with pressure profiles and obtained agreement with measurements for $2a/\lambda \leqslant 0{\cdot}06$.

Consequently we conclude that a good approximation of the pressure variation, the velocity field outside the viscous wall region and the first harmonic of the shear-stress variation for waves on which there is not a large separated ragion can be obtained

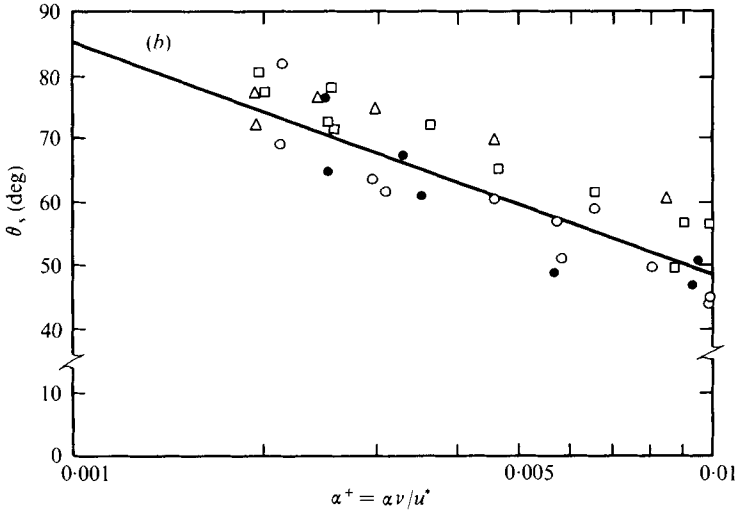

FIGURE 11. Comparison of model D with (*a*) experimental magnitude of shear-stress variation and (*b*) experimental shear-stress phase angles. ——, model D; ●, $2a/\lambda = 0{\cdot}0114$; ○, $2a/\lambda = 0{\cdot}0125$; □, $2a/\lambda = 0{\cdot}0312$; △, $2a/\lambda = 0{\cdot}050$.

by a solution of the linear momentum equations. However, it should be pointed out that the agreement between calculations and measurements does not provide a confirmation of the model of the wave-induced Reynolds stresses used by Thorsness. It is quite likely that other models would also provide the type of agreement between linear theory and presently available measurements shown in this paper and the thesis by Thorsness (1975). In fact, Thorsness has discussed this matter in great detail and has shown that the use of his model D with constants $k_1 = -30$, $k_{LP} = 1500$ and $k_{L\tau} = 0$ gives results very close to the ones presented in this paper.

This work was supported by the National Science Foundation under Grant NSF ENG 71-02362.

REFERENCES

BEAVERS, G. S., SPARROW, E. M. & LLOYD, R. J. 1971 *J. Basic Engng* **93**, 296.

BENJAMIN, T. B. 1959 *J. Fluid Mech.* **6**, 161.

BLINCO, P. H. & SANDBORN, V. A. 1973 *Proc. Symp. Turbulence in Liquids, Univ. Missouri – Rolla.*

BONCHKOVSKAYA, T. V. 1955 *Akad. Nauk SSSR, Morskoi Gidrofiz. Inst.* **6**, 98.

CLARK, J. A. 1968 *Dept. Mech. Engng, Queen's Univ. Belfast Rep.* no. 253.

COOK, G. W. 1970 Turbulent flow over solid wavy surfaces. Ph.D. thesis, Dept. Chemical Engineering, University of Illinois, Urbana.

DIMOPOULOS, H. & HANRATTY, T. J. 1968 *J. Fluid Mech.* **33**, 303.

FORTUNA, G. & HANRATTY, T. J. 1971 *Int. J. Heat Mass Transfer* **14**, 1499.

HANRATTY, T. J. 1967 *Phys. Fluids Suppl.* **10**, 5126.

HELMHOLTZ, H. 1868 *Mber. preuss Akad. Wiss.* **24**, 215.

HUSSAIN, A. K. M. F. & REYNOLDS, W. C. 1970 *Thermosci. Div., Stanford Univ. Rep.* FM-6.

JOLLS, K. R. & HANRATTY, T. J. 1969 *A.I.Ch.E. J.* **15**, 199.

KLINE, S. J., MORKOVIN, M. V. & COCKRELL, D. J. 1969 *Comp. Turbulent Boundary Layers*: 1968 *ASSOR – IFP – Stanford Conf. Thermosci. Div., Stanford Univ.*

LARRAS, J. & CLARIA, A. 1960 *Houille Blanche* **6**, 674.

LOYD, R. J., MOFFAT, R. J., & KAYS, W. M. 1970 *Thermosci. Div., Stanford Univ. Rep.* HMT-13.

MITCHELL, J. E. & HANRATTY, T. J. 1966 *J. Fluid Mech.* **26**, 199.

MORRISROE, P. E. 1970 Flow over solid wavy surfaces. M.S. thesis, Dept. Chemical Engineering, University of Illinois, Urbana.

MOTZFIELD, H. 1937 *Z. angew. Math. Mech.* **17**, 193.

PATEL, V. C. & HEAD, M. R. 1969 *J. Fluid Mech.* **38**, 181.

SAEGER, J. C. & REYNOLDS, W. C. 1971 *Thermosci. Div., Stanford Univ. Rep.* FM-9.

SHAW, D. A. 1976 Mechanism of turbulent mass transfer to a pipe wall at high Schmidt numbers. Ph.D. thesis, Dept. Chemical Engineering, University of Illinois, Urbana.

SIGAL, A. 1971 Ph.D. thesis, Dept. Aeronautical Engineering, California Institute of Technology.

SIRKAR, K. K. & HANRATTY, T. J. 1970 *J. Fluid Mech.* **44**, 605.

SON, J. S. & HANRATTY, T. J. 1969 *J. Fluid Mech.* **35**, 353.

THORSNESS, C. B. 1975 Transport phenomena associated with flow over a solid wavy surface. Ph.D. thesis, Dept. Chemical Engineering, University of Illinois, Urbana.

THORSNESS, C. B. & HANRATTY, T. J. 1977 Turbulent flow over wavy surfaces. In *Proc. Symp. Turbulent Flows, Pennsylvania State Univ.*

ZAGUSTIN, K., HSU, E. Y., STREET, R. L. & PERRY, B. 1966 *Dept. Civil Engng, Stanford Univ. Tech. Rep.* no. 60.

ZILKER, D. P. 1972 Flow over wavy surfaces. M.S. thesis. Dept. Chemical Engineering, University of Illinois, Urbana.

ZILKER, D. P. 1976 Flow over wavy surfaces. Ph.D. thesis, Dept. Chemical Engineering, University of Illinois, Urbana.